

## Doping effect on orthorhombic $\text{Sr}_2\text{VO}_4$ with $s = \frac{1}{2}$ dimers

K. Funahashi,<sup>1</sup> T. Higashide,<sup>1</sup> T. Ueno,<sup>1</sup> K. Tasaki,<sup>1</sup> Y. Tahara,<sup>1</sup> M. Adachi,<sup>1</sup> T. Saiki,<sup>1</sup> T. Kajita,<sup>1</sup> and T. Katsufuji<sup>1,2</sup>

<sup>1</sup>*Department of Physics, Waseda University, Tokyo 169-8555, Japan*

<sup>2</sup>*Kagami Memorial Research Institute for Materials Science and Technology, Waseda University, Tokyo 169-0051, Japan*



(Received 1 September 2018; revised manuscript received 11 October 2018; published 20 November 2018)

We studied single crystals of orthorhombic  $\text{Sr}_2\text{VO}_4$  containing spin-singlet dimers of  $\text{V}^{4+}$  ( $3d^1$ ) and those with Ti or Nb substituted for V. We found that both Ti and Nb dopings induce the evolution of a Curie-Weiss component in the magnetic susceptibility, but the rate of evolution with doping is several times higher for Nb doping. We also found that Nb doping induces the conduction of  $d$  electrons. These results can be explained by the hybridization of the Nb  $4d$  states with the  $3d$  states of the neighboring V ions, possibly causing rearrangement of the  $d$  electron in the doubly degenerate  $e$  states in the V ion.

DOI: [10.1103/PhysRevB.98.184422](https://doi.org/10.1103/PhysRevB.98.184422)

### I. INTRODUCTION

Spin-dimer systems are one of the simplest systems with a spin-singlet ground state. There are several examples of the spin-dimer systems that exhibit spin-gap behavior in the temperature ( $T$ ) dependence of magnetic susceptibility, indicating a spin-singlet ground state [1–8]. In several compounds, neutron inelastic scattering has been measured, and a spin-gap structure has been observed in the spin-excitation spectrum [3,9–11]. In addition, the magnetization or spin-excitation spectrum under the application of a strong magnetic field has been measured in some of the compounds, and characteristic behaviors arising from the spin-singlet ground state have been observed [2,4,7,8,12,13].

One of the intriguing issues regarding the spin-gap state is how it changes with doping. For example, the appearance of antiferromagnetic ordering when nonmagnetic impurities are introduced into a spin-singlet ground state has been observed experimentally in some compounds [14,15], although there have been a limited number of studies on this issue probably because of the lack of compounds suitable for study.

$\text{Sr}_2\text{VO}_4$  with  $\text{V}^{4+}$  ( $3d^1$  electron configuration) is known to have two polymorphs. One has the  $\text{K}_2\text{NiF}_4$  structure with a tetragonal lattice of  $\text{V}^{4+}$  ions [16–28]. This compound exhibits successive structural phase transitions at  $\sim 100$  K but does not exhibit magnetic ordering, and its possible exotic orbital ordering has been discussed. However, this tetragonal phase is stable only in a limited range of the temperature and oxygen partial pressure during the synthesis, and an orthorhombic phase is more stable under a wider range of conditions [29,30]. In this orthorhombic phase,  $\text{V}^{4+}$  ions form a hexagonal-closed-packed- (hcp-) like structure where two inequivalent triangular lattices of V ions stack alternately along the  $a$  axis of the orthorhombic structure as illustrated in Fig. 1(a). There are six inequivalent bonds connecting the V ions in the neighboring layers, denoted by (1)–(6) in Fig. 1(a), and one of them (shown by thick lines) is shorter than the others, corresponding to a V dimer. As a result, all the V ions form a dimer in this crystal structure. Each V ion is surrounded by four oxygen ions in a nearly tetrahedral

configuration with no overlap with those surrounding the neighboring V ions [Fig. 1(c)]. This orthorhombic  $\text{Sr}_2\text{VO}_4$  exhibits typical spin-gap behavior in the  $T$  dependence of the magnetic susceptibility, which arises from the spin-singlet state on the short V-V bonds (V dimers) [29,30].

In the present paper, we grew single crystals of orthorhombic  $\text{Sr}_2\text{VO}_4$  with V dimers and those with part of the V ions substituted by Ti or Nb and studied how the magnetic, transport and optical properties of the compounds change with doping. We found that Nb doping causes the evolution of a Curie-Weiss component in the magnetic susceptibility of which the rate cannot be explained by a doping of localized nonmagnetic impurities. We also found that Nb doping induces the electrical conduction. These results can be discussed in terms of the hybridization of the  $4d$  orbitals of Nb ions with the  $3d$  orbitals of the neighboring V ions.

### II. EXPERIMENT

For the single-crystal growth of  $\text{Sr}_2\text{VO}_4$ , strontium oxide (SrO), which was obtained by heating  $\text{SrCO}_3$  at  $1000^\circ\text{C}$  for 12 h, and  $\text{V}_2\text{O}_3$  with a Sr:V molar ratio of 2:1 were mixed and left in air for several days. During this process, the SrO appeared to absorb water in the air, and the powder became sticky. Then the powder was pressed into a rod and sintered in a floating-zone furnace in a flow of  $\text{H}_2$  7%/Ar gas slightly below its melting temperature. The sintered rod was ground and pressed into a rod again, and a single crystal was grown by melting the rod in the floating-zone furnace in a flow of  $\text{H}_2$  7%/Ar gas. For the Ti- and Nb-doped crystals, the same method was employed with  $\text{TiO}_2$  or  $\text{Nb}_2\text{O}_5$  as a starting material. The typical size of the crystals is 5 mm in diameter and 3 cm in length. Some of the grown crystals were hygroscopic and broke into pieces over a period of hours to months. We speculate that a small amount of SrO remaining as an impurity inside the grown crystal absorbed water and was responsible for the deterioration of the crystals. For  $\text{Sr}_2\text{V}_{1-x}\text{Ti}_x\text{O}_4$ ,  $x$  can be increased to  $\sim 0.2$  but for  $\text{Sr}_2\text{V}_{1-x}\text{Nb}_x\text{O}_4$ , a  $\text{K}_2\text{NiF}_4$  phase appeared as an impurity phase when  $x$  was larger than 0.05. We measured the x-ray powder diffraction of the

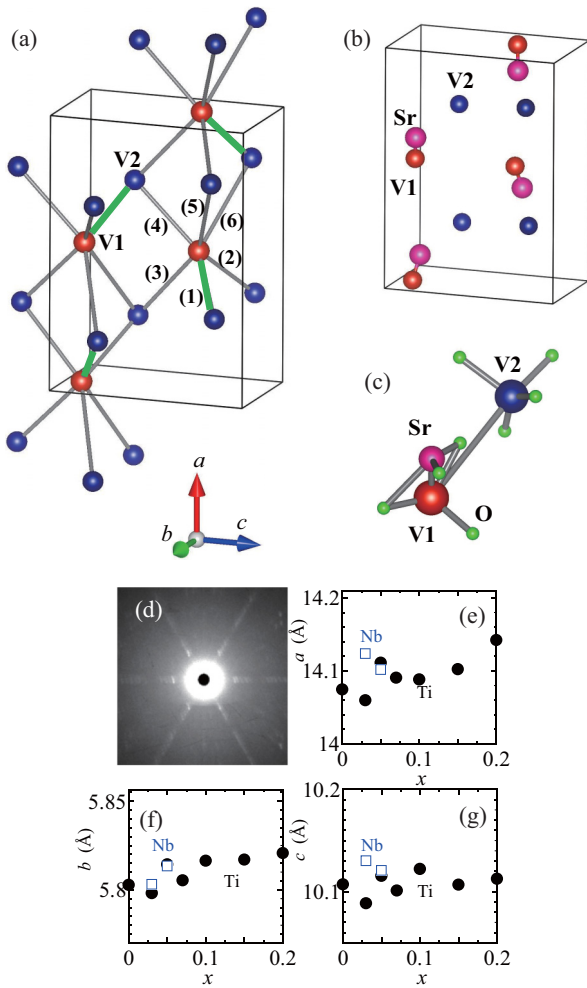


FIG. 1. Atomic positions of (a) V ions, (b) V ions and Sr ions, and (c) V ions in a dimer, a Sr ion, and oxygen ions in orthorhombic  $\text{Sr}_2\text{VO}_4$ . The thick lines in (a) represent the shortest V-V bonds forming a spin-singlet dimer. The data of the atomic positions are from Ref. [29]. The pictures were drawn by VESTA [31]. (d) A Laue photograph on the  $bc$  plane of  $\text{Sr}_2\text{V}_{0.95}\text{Nb}_{0.05}\text{O}_4$ . (e)–(g)  $x$  dependence of the lattice constants.

crushed single crystals, and the lattice constants obtained by the analysis are shown in Figs. 1(e)–1(g). The  $a$  and  $b$  lattice constants increase slightly with Ti doping.

The orientation of the crystals was determined by the Laue method [Fig. 1(d)]. The amounts of Sr, V, Ti, and Nb were determined by induction-coupled plasma (ICP) analysis, and the results are summarized in Table I [32]. Magnetic susceptibility was measured by a superconducting quantum interference device magnetometer with an applied magnetic field of 0.1 T. Resistivity was measured by the two-probe technique with an electrometer for the undoped sample with high resistivity and by the four-probe technique for the Nb-doped sample with relatively low resistivity. Thermopower was measured by the conventional steady-state method. Optical reflectivity on the polished surface of the crystal was measured by a grating spectrometer between 0.7 and 5 eV and by a Fourier transform infrared spectrometer between 0.08 and 0.8 eV. An Al mirror

TABLE I. Amounts of Sr, V, Ti, and Nb in the crystals determined by ICP.

$x$	Sr	V	Ti
0	1.98	1.00	0.00
0.03	1.97	0.97	0.03
0.05	1.97	0.95	0.05
0.07	1.94	0.93	0.07
0.10	2.00	0.90	0.10
0.15	1.98	0.85	0.15
0.20	1.95	0.80	0.20
$x$	Sr	V	Nb
0.03	1.97	0.97	0.03
0.05	1.97	0.95	0.05

with known reflectivities was used as a reference for obtaining the reflectivity.

### III. RESULTS AND DISCUSSIONS

Figure 2(a) shows the  $T$  dependence of the magnetic susceptibility  $\chi$  for orthorhombic  $\text{Sr}_2\text{VO}_4$  with the magnetic field applied along the  $a$ ,  $b$ , and  $c$  axes. A peak exists in  $\chi(T)$  at  $\sim 50$  K for all the data, which is almost the same as that for the polycrystalline samples previously reported [29,30]. Hardly any anisotropy of  $\chi(T)$  exists.

Figure 2(b) shows  $\chi(T)$  for the Ti-doped samples,  $\text{Sr}_2\text{V}_{1-x}\text{Ti}_x\text{O}_4$ , with an unknown direction of the magnetic

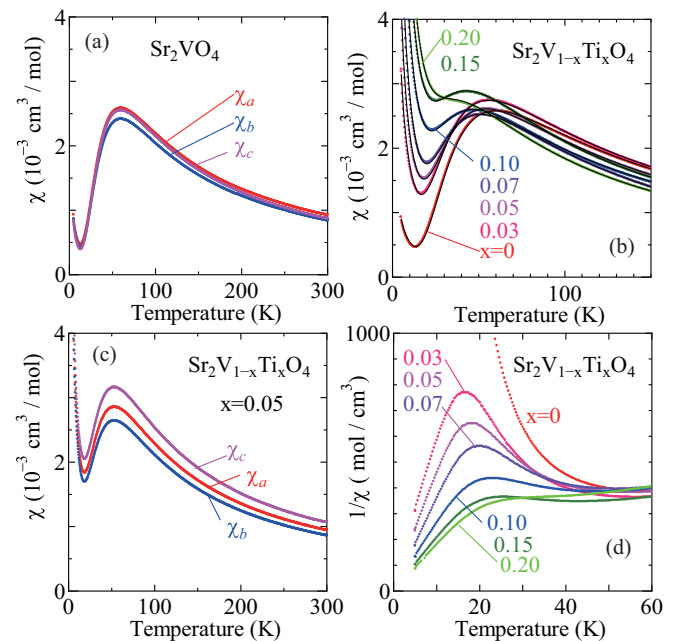


FIG. 2. Temperature dependence of the magnetic susceptibility (a) for  $\text{Sr}_2\text{VO}_4$  with the magnetic field applied along the  $a$ ,  $b$ , and  $c$  axes, (b) for  $\text{Sr}_2\text{V}_{1-x}\text{Ti}_x\text{O}_4$  with various values of  $x$  for an unknown direction of the magnetic field, (c) for  $\text{Sr}_2\text{V}_{1-x}\text{Ti}_x\text{O}_4$  with  $x = 0.05$  with the magnetic field applied along the  $a$ ,  $b$ , and  $c$  axes, and (d) inverse magnetic susceptibility for  $\text{Sr}_2\text{V}_{1-x}\text{Ti}_x\text{O}_4$  with various values of  $x$ . The solid lines in (b) are the results of the fitting.

field. As can be seen, the magnitude of the low- $T$  Curie component gradually increases with increasing Ti concentration  $x$ , although the peak at  $\sim 50$  K barely changes. Figure 2(c) shows  $\chi(T)$  for  $x = 0.05$  with the magnetic field along the three different axes. There is also hardly any anisotropy in  $\chi(T)$  in the Ti-doped samples. To observe the Curie component more clearly, the inverse magnetic susceptibility  $1/\chi$  is plotted as a function of  $T$  in Fig. 2(d). A linear  $T$  dependence of  $1/\chi(T)$  below 15 K and a decrease in the slope with increasing  $x$  are clearly observed.

The spin-gap formula of  $\chi(T)$  for the  $s = 1/2$  dimer system was first discussed by Bleaney and Bowers [1], which is given as

$$\chi_{\text{SG}}(T) = \frac{C_1}{T(1 + \frac{1}{3} \exp(J/k_B T))}, \quad (1)$$

where  $J$  corresponds to the excitation energy from the spin-singlet ground state to the spin-triplet excited state for the  $V^{4+}$  ( $3d^1$ ) dimer with an antiferromagnetic interaction. The coefficient  $C_1$  for the parent compound Sr<sub>2</sub>VO<sub>4</sub>,  $C_1^p$  is theoretically given by

$$C_1^p = \frac{Ns^2g^2\mu_B^2}{k_B}, \quad (2)$$

where  $N$  is the number of V sites with  $s = 1/2$  spins,  $g$  is the  $g$  factor ( $\sim 2$ ), and  $\mu_B$  is the Bohr magneton. We fitted the experimentally obtained  $\chi(T)$  with the sum of  $\chi_{\text{SG}}(T)$ , the Curie-Weiss component  $\chi_{\text{CW}}(T)$ , and a  $T$ -independent component  $\chi_0$ ,

$$\chi(T) = \chi_{\text{SG}}(T) + \chi_{\text{CW}}(T) + \chi_0, \quad (3)$$

where

$$\chi_{\text{CW}}(T) = \frac{C_2}{T + \theta}. \quad (4)$$

Note that there are five parameters ( $C_1$ ,  $J$ ,  $C_2$ ,  $\theta$ , and  $\chi_0$ ) in this formula. The results of the fitting are shown by solid lines in Fig. 2(b). The  $x$  dependence of the parameters is shown in Fig. 3 by solid circles. As can be seen, the magnitude of the Curie-Weiss component  $C_2$  increases, whereas that of the spin-gap component  $C_1$  decreases and the size of the spin gap  $J$  barely changes with increasing Ti concentration  $x$ .

To understand the increase in  $C_2$  and the decrease in  $C_1$  with Ti doping, let us consider the following model. We assume that the valence of Ti is 4+ and that there are no  $d$  electrons in Ti. If  $\text{Ti}^{4+}$  ( $3d^0$ ) is substituted for one of the two  $V^{4+}$  ( $3d^1$ ) ions in a spin-singlet dimer, a  $s = \frac{1}{2}$  spin appears, and if the magnetic interactions of this spin with the other V spins are sufficiently small, a Curie-Weiss term with a low Weiss temperature  $\theta$  (which has been experimentally shown to be several kelvins) should appear. However, the fact that, if both V sites are substituted by Ti, then no Curie-Weiss term appears must be taken into account. For Sr<sub>2</sub>V<sub>1-x</sub>Ti<sub>x</sub>O<sub>4</sub>, the probability that only one of the V ions in the dimer is substituted by Ti, the probability that both are substituted by Ti, and the probability that neither of them are substituted by Ti are  $2x(1-x)$ ,  $x^2$ , and  $(1-x)^2$ , respectively. Therefore,

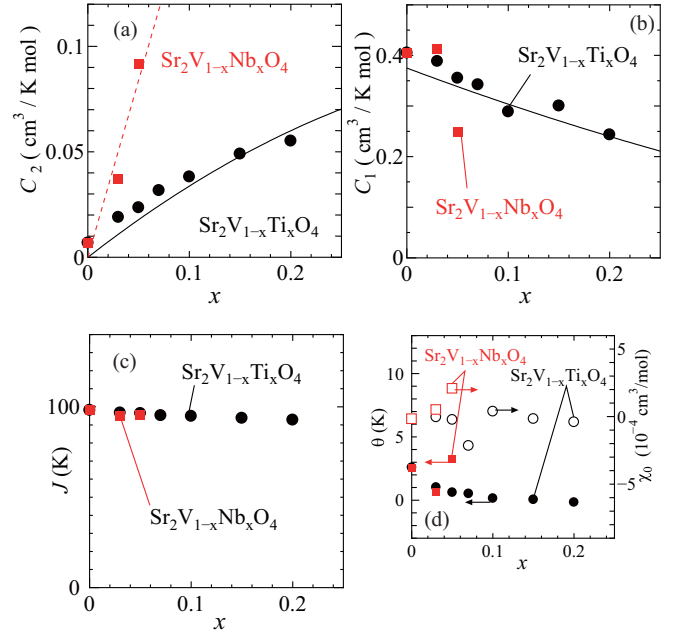


FIG. 3. Dependence on the dopant (Ti or Nb) concentration ( $x$ ) of (a)  $C_2$  (the magnitude of the Curie-Weiss component), (b)  $C_1$  (the magnitude of the spin-gap component), (c)  $J$  (the size of the spin gap), and (d)  $\theta$  (the Weiss temperature) and  $\chi_0$  (the  $T$ -independent component) for Sr<sub>2</sub>V<sub>1-x</sub>Ti<sub>x</sub>O<sub>4</sub> (circles) and Sr<sub>2</sub>V<sub>1-x</sub>Nb<sub>x</sub>O<sub>4</sub> (squares). For each parameter, see Eqs. (1)–(4). The solid lines in (a) and (b) represent the theoretical curves given by Eqs. (5) and (6), respectively. The dashed line in (a) is a guide to the eyes.

the magnitudes of the Curie-Weiss term and the spin-gap term are given by [33]

$$C_2 = x(1-x) \frac{Ns^2g^2\mu_B^2}{k_B}, \quad (5)$$

$$C_1 = (1-x)^2 \frac{Ns^2g^2\mu_B^2}{k_B}. \quad (6)$$

We plot the  $x$  dependences of  $C_2$  and  $C_1$  given by Eqs. (5) and (6) as solid lines in Figs. 3(a) and 3(b), respectively. As can be seen, the experimental results are in good agreement with the theoretical curves. Together with the fact that  $J$  hardly changes with  $x$  [Fig. 3(c)], it can be concluded that the Ti ion introduced into the  $s = \frac{1}{2}$  dimer acts as a localized  $s = 0$  ion.

We also measured  $\chi(T)$  for the Nb-doped samples as shown in Fig. 4. The results are qualitatively the same as those for the Ti-doped samples, although the evolution of the Curie-Weiss term with  $x$  is much faster for the Nb-doped samples. We also fitted  $\chi(T)$  with Eq. (3) and plot  $C_2$  and  $C_1$  as functions of  $x$  by closed squares in Figs. 3(a) and 3(b), respectively. As can be seen,  $C_2$  increases much faster with Nb doping than with Ti doping. This indicates that the Nb ion introduced to the V dimer network does not act as a simple localized  $s = 0$  ion but affects the neighboring V dimers, resulting in the simultaneous suppression of many singlet dimers in Sr<sub>2</sub>V<sub>1-x</sub>Nb<sub>x</sub>O<sub>4</sub>. Note that hardly any anisotropy

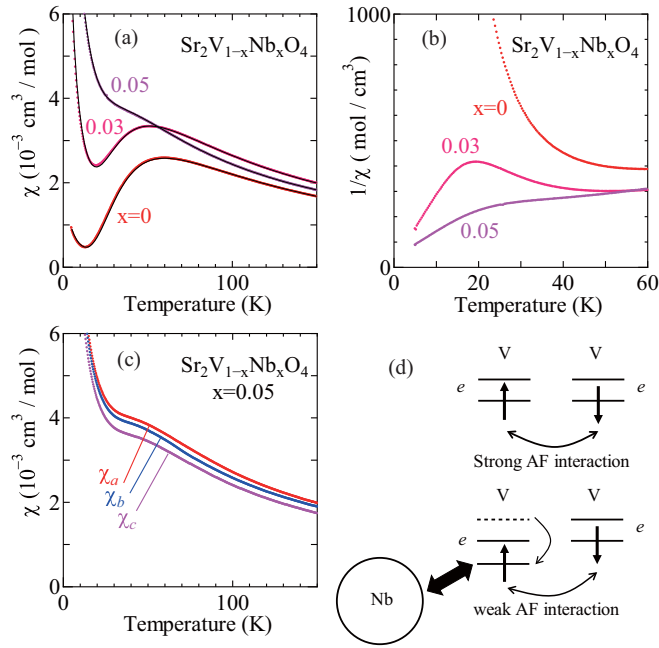


FIG. 4. Temperature dependence of (a) the magnetic susceptibility and (b) the inverse magnetic susceptibility for  $\text{Sr}_2\text{V}_{1-x}\text{Nb}_x\text{O}_4$  with various values of  $x$  in an unknown direction of the magnetic field and of (c) the magnetic susceptibility for  $\text{Sr}_2\text{V}_{1-x}\text{Nb}_x\text{O}_4$  with  $x = 0.05$  with the magnetic field applied along the  $a$ ,  $b$ , and  $c$  axes. The solid lines in (a) are the results of the fitting. (d) Schematic of the electronic state in the V dimer without and with Nb doping at a nearby site.

in  $\chi(T)$  also exists in the Nb-doped samples as shown in Fig. 4(c).

The temperature dependence of the resistivity  $\rho$  for  $\text{Sr}_2\text{VO}_4$  and the Nb-doped samples is shown in Fig. 5. For  $\text{Sr}_2\text{VO}_4$ ,  $\rho$  is on the order of  $10^7 \Omega \text{ cm}$  at room temperature irrespective of the direction and further increases with decreasing  $T$ . The activation energy of  $\text{Sr}_2\text{VO}_4$  estimated from  $\rho(T)$  is  $\sim 0.5 \text{ eV}$ . On the other hand,  $\rho$  for  $\text{Sr}_2\text{V}_{1-x}\text{Nb}_x\text{O}_4$  with  $x = 0.05$  at room temperature is many orders of magni-

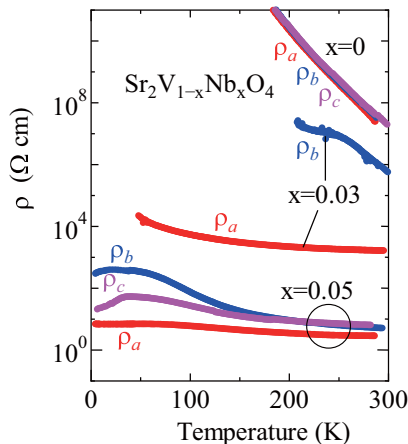


FIG. 5. Temperature dependence of the resistivity for  $\text{Sr}_2\text{V}_{1-x}\text{Nb}_x\text{O}_4$ .

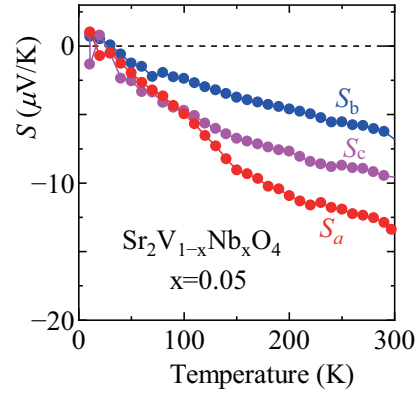


FIG. 6. Temperature dependence of the Seebeck coefficient for  $\text{Sr}_2\text{V}_{1-x}\text{Nb}_x\text{O}_4$  with  $x = 0.05$ .

tude smaller than that for the parent compound, and furthermore, it does not diverge at the lowest  $T$ , although a slight increase with decreasing  $T$  is observed. Note that there is clear anisotropy in the resistivity of the Nb-doped crystals;  $\rho_a$  is lower than  $\rho_b$  and  $\rho_c$ .

To further confirm the conducting state in the Nb-doped sample, the Seebeck coefficient  $S$  for  $\text{Sr}_2\text{V}_{1-x}\text{Nb}_x\text{O}_4$  with  $x = 0.05$  was measured as shown in Fig. 6.  $S$  is negative, and its absolute value decreases with decreasing  $T$ , a typical behavior of a metallic state. From these results, it can be concluded that Nb doping in orthorhombic  $\text{Sr}_2\text{VO}_4$  results in a conducting state.

Figures 7(a) and 7(b), respectively, show the optical reflectivity spectra below 5 eV at room temperature for  $\text{Sr}_2\text{VO}_4$  and  $\text{Sr}_2\text{V}_{1-x}\text{Nb}_x\text{O}_4$  with  $x = 0.05$ . Several structures below

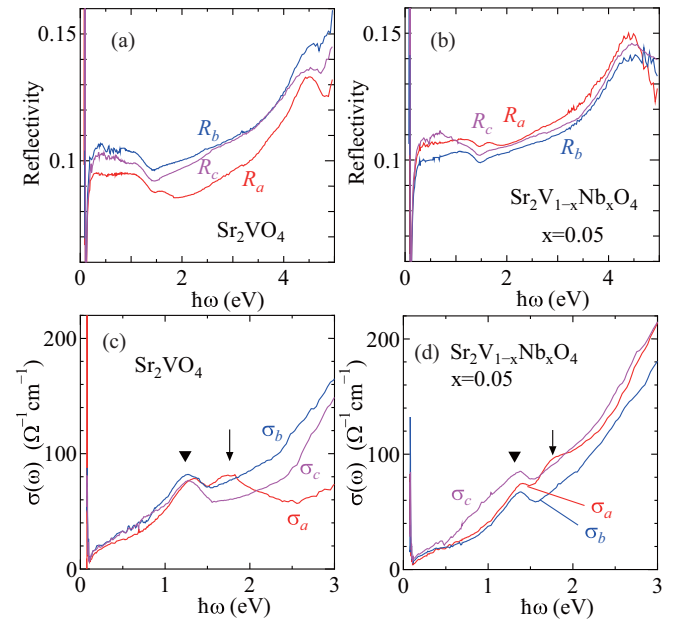


FIG. 7. (a) and (b) Optical reflectivity spectra and (c) and (d) optical conductivity spectra for (a) and (c)  $\text{Sr}_2\text{VO}_4$  and (b) and (d)  $\text{Sr}_2\text{V}_{1-x}\text{Nb}_x\text{O}_4$  with  $x = 0.05$  with polarization along the  $a$ ,  $b$ , and  $c$  axes.

2 eV and a peak at 4.5 eV are observed in all the polarization spectra of both compounds. The peak at 4.5 eV can be assigned to the charge-transfer excitation from the oxygen  $2p$  state to the V  $3d$  state. We performed a Kramers-Kronig transformation of the reflectivity spectra and obtained the optical conductivity [ $\sigma(\omega)$ ] spectra shown in Figs. 7(c) and 7(d) [34]. We found, however, that the spectrum below 3 eV depends on the way of extrapolation of the reflectivity spectra above 5 eV to the extent that the uncertainty arising from the extrapolation exceeds the difference in the spectra associated with Nb doping. Accordingly, a quantitative discussion of the dependence of the optical conductivity spectra on Nb doping is difficult.

In all the polarization  $\sigma(\omega)$  spectra obtained both with and without Nb dopings, a peak at 1.2 eV [shown by triangles in Figs. 7(c) and 7(d)] and a broad background from 0 to 3 eV are observed. On the basis of a previous result on the optical spectrum of VO<sub>2</sub> having V<sup>4+</sup> similar to the present compound [35], the broad background can be assigned to Mott-gap excitation between the neighboring V  $3d$  states. On the other hand, the peak at 1.2 eV can be assigned to intraatomic excitation within the V  $3d$  states (crystal-field excitation) [36]. In the present compound, V is surrounded by four oxygen ions in the tetrahedral configuration, accordingly, the doubly degenerate  $e$  states have a lower energy than the triply degenerate  $t_2$  states, and a  $d$  electron is accommodated in one of the  $e$  states. Thus, the peak at 1.2 eV can be assigned to the intraatomic excitation from the  $e$  state to the  $t_2$  state of the V ions.

One of the differences in the optical spectra with and without Nb dopings is the anisotropy of the spectra. For the parent compound, the reflectivity in the case of polarization along the  $b$  axis ( $R_b$ ) is higher than that along the other axes but for the Nb-doped compound,  $R_b$  is lower than the  $R_a$  and  $R_c$ . As a result, the increase in the reflectivity with Nb doping is greatest for  $R_a$ . This is also the case for the  $\sigma(\omega)$  spectrum and is consistent with the lower resistivity (higher conductivity) along the  $a$  axis in the Nb-doped samples as experimentally observed (Fig. 5).

Another characteristic of the optical spectra is that, in addition to the peak at 1.2 eV observed in all the polarization spectra, a peak at 1.7 eV [shown by arrows in Figs. 7(c) and 7(d)] exists only in the  $\sigma_a(\omega)$  spectrum for both the undoped and the Nb-doped samples. Note that the corresponding structure also exists in the reflectivity spectrum along the  $a$  polarization direction. Although the  $a$  axis is a special direction for the hcp lattice of V ions, none of the V-V bonds are along the  $a$  axis as shown in Fig. 1(a). Furthermore, for the VO<sub>4</sub> tetrahedra, the  $a$  axis is not a special axis as shown in Fig. 1(c). On the other hand, one of the four inequivalent Sr ions exists close to one of the two inequivalent V ions, forming a V-Sr bond with a length of only 1.5 Å, and the direction of the bond is almost along the  $a$  axis as illustrated in Fig. 1(b). Thus, a possible origin of the structure at 1.7 eV in the  $\sigma_a(\omega)$  spectrum is the Sr ion existing near the V ion affecting the  $d$  orbital of the V ion, resulting in excitation only when the polarization is along the V-Sr direction.

Let us consider how the doped Nb ions act in the orthorhombic Sr<sub>2</sub>VO<sub>4</sub>. The main difference between Ti and Nb is that Ti<sup>4+</sup> is  $d^0$  whereas Nb<sup>5+</sup> is  $d^0$ . Thus, one idea is that

the substitution of Nb<sup>5+</sup> for V<sup>4+</sup> results in the electron doping into V<sup>4+</sup>. Note that a doping effect on Sr<sub>2</sub>VO<sub>4</sub> with a K<sub>2</sub>NiF<sub>4</sub> structure by the introduction of oxygen off stoichiometry [23,26] or the substitution of H<sup>-</sup> for O<sup>2-</sup> [27] has been studied previously. However, in the present compound, the doping effect only cannot explain the greater evolution of the Curie-Weiss term with Nb than Ti doping. Namely, the electron doping into V<sup>4+</sup> may enhance a Pauli paramagnetic susceptibility but does not cause the Curie-Weiss term since it is difficult to break the spin-singlet V-V bonds but to keep the two V spins localized by electron doping. Furthermore, it is unlikely that only the 5% electron doping alone to the Mott insulator with a resistivity of more than 10<sup>7</sup> Ω cm at room temperature results in the conducting ground state since there is an empirical rule that Mott insulators with higher resistivities require a large number of doped carriers to make them conducting. Indeed, various  $3d$  transition-metal oxides with perovskite structures have been studied [37–39] and found that even if the resistivity of the undoped sample (a Mott insulator) is on the order of 10<sup>1</sup> Ω cm at room temperature, the resistivity of the sample with 5% doping usually diverges at the lowest  $T$ .

Thus, it is more likely that the  $4d$  orbital of the Nb ion extending in a wider range in space and thus being strongly hybridized with the  $3d$  orbitals of the V ions at the neighboring sites plays an important role both for magnetism and transport properties. In other words, the doped Nb ions act not only as donors, but also as increasing the bandwidth. However, it may be difficult to break the spin-singlet V-V bond and to create two  $s = \frac{1}{2}$  spins only by increasing the hybridization between the V  $3d$  orbital and the Nb  $4d$  orbital. One possible scenario is that the occupation of the  $d$  electron in the V ion changes with the Nb doping to a neighboring V site [Fig. 4(d)]. The strong antiferromagnetic interaction within the V-V dimers in the parent compound indicates that one of the doubly degenerate  $e$  states of one V ion forms a strong bond with an  $e$  state in the other V ion in the dimer. However, the unoccupied  $e$  state in the V ion can be hybridized with the  $4d$  state of the neighboring Nb, and its energy can be lowered as a consequence. As a result, in the Nb-doped sample, it is possible that the  $d$  electron in the V ion now occupies the state that was unoccupied in the parent compound and the strong antiferromagnetic interaction between the V ions no longer exists. Such rearrangement of the electron in the  $e$  state associated with Nb doping at a nearby site can explain the faster suppression of the spin-singlet state in the Nb-doped samples.

Let us also consider the origin of the larger conductivity along the  $a$  axis when Nb ions are doped. As discussed in the Introduction, there are various inequivalent V-V bonds in the present compound. Among them, a spin-singlet state exists on the shortest bond with a length of 4.08 Å as shown in Fig. 1(a). With Nb doping, however, the  $4d$  orbital existing in the doped Nb is hybridized with the  $3d$  orbitals of the neighboring V ions, causing the conductivity of the Nb-doped samples. Regarding the V-V bonds in the quasi-hcp lattice of the V ions, there are five different V-V bonds, which are denoted as V-( $n$ )-V with  $n = 2-6$  in addition to the shortest V-V bond denoted as V-(1)-V [Fig. 1(a)]. If we consider the chains of V ions V-(1)-V-( $n$ )-V-(1)-V-( $n$ )-... ( $n = 2-6$ ), two of them

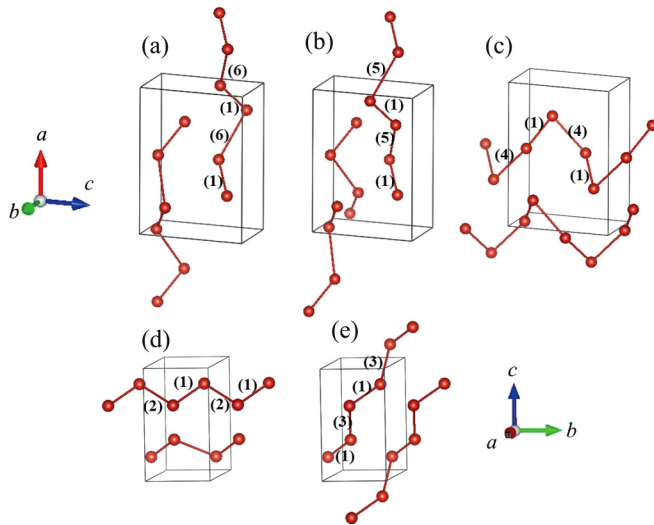


FIG. 8. Chains of V ions including the shortest V-V bonds [annotated as (1)] in orthorhombic  $\text{Sr}_2\text{VO}_4$ . The annotation of the bonds ( $n$ ) is the same as that in Fig. 1(a).

are along the  $a$  axis [Figs. 8(a) and 8(b)], one is along the  $c$  axis [Fig. 8(c)], one is along the  $b$  axis [Fig. 8(d)], and the other one is along the  $\langle 011 \rangle$  direction [Fig. 8(e)]. This means that the number of chains containing the shortest V-V bonds is largest along the  $a$  axis, and this can explain why the conductivity along the  $a$  axis is larger for the sample with Nb doping.

#### IV. SUMMARY

We grew single crystals of orthorhombic  $\text{Sr}_2\text{VO}_4$  composed of spin-singlet  $\text{V}^{4+}$  ( $3d^1$ ) dimers and those with Ti or Nb substituted for the V site and studied their magnetic, transport, and optical properties. Regarding the spin-gap behavior in the magnetic susceptibility of the parent compound, a Curie-Weiss component evolves with the doping of Ti and Nb. The rate of evolution of the Curie-Weiss component with the Ti doping is quantitatively consistent with a model in which the nonmagnetic localized  $\text{Ti}^{4+}$  ion is substituted for  $\text{V}^{4+}$  in the spin-singlet dimer, whereas the rate for Nb doping is several times higher than that for Ti doping. We also found that Nb doping to the V site results in an electrically conducting state. These experimental results suggest that the  $4d$  state of the Nb ion is hybridized with the  $3d$  state of the neighboring V ion. This causes possible rearrangement of the electron in the  $e$  state of the V ion, resulting in the disappearance of the strong antiferromagnetic interaction within the V dimers. We also found from resistivity and optical measurements that the Nb-doped sample has higher conductivity along the  $a$  direction and this can be understood from the V-V network in the crystal.

#### ACKNOWLEDGMENTS

This work was supported by JST CREST Grant No. JP-MJCR15Q2 and by JSPS KAKENHI Grant No. 16H04020. K.F. acknowledges the Leading Graduate Program in Science and Engineering, Waseda University from MEXT, Japan.

- [1] B. Bleaney and K. D. Bowers, *Proc. R. Soc. London, Ser. A* **214**, 451 (1952).
- [2] Y. Sasago, M. Hase, K. Uchinokura, M. Tokunaga, and N. Miura, *Phys. Rev. B* **52**, 3533 (1995).
- [3] Y. Sasago, K. Uchinokura, A. Zheludev, and G. Shirane, *Phys. Rev. B* **55**, 8357 (1997).
- [4] T. Nikuni, M. Oshikawa, A. Oosawa, and H. Tanaka, *Phys. Rev. Lett.* **84**, 5868 (2000).
- [5] J. Deisenhofer, R. M. Eremina, A. Pimenov, T. GavriloVA, H. Berger, M. Johnsson, P. Lemmens, H.-A. K. von Nidda, A. Loidl, K.-S. Lee *et al.*, *Phys. Rev. B* **74**, 174421 (2006).
- [6] R. M. Eremina, T. P. GavriloVA, A. Günther, Z. Wang, R. Lortz, M. Johnsson, H. Berger, H. A. K. von Nidda, J. Deisenhofer, and A. Loidl, *Eur. Phys. J. B* **84**, 391 (2011).
- [7] A. A. Aczel, Y. Kohama, M. Jaime, K. Ninios, H. B. Chan, L. Balicas, H. A. Dabkowska, and G. M. Luke, *Phys. Rev. B* **79**, 100409(R) (2009).
- [8] A. A. Aczel, Y. Kohama, C. Marcenat, F. Weickert, M. Jaime, O. E. Ayala-Valenzuela, R. D. McDonald, S. D. Selesnic, H. A. Dabkowska, and G. M. Luke, *Phys. Rev. Lett.* **103**, 207203 (2009).
- [9] Ch. Rüegg, D. F. McMorrow, B. Normand, H. M. Ronnow, S. E. Sebastian, I. R. Fisher, C. D. Batista, S. N. Gvasaliya, Ch. Niedermayer, and J. Stahn, *Phys. Rev. Lett.* **98**, 017202 (2007).
- [10] Ch. Rüegg, N. Cavadini, A. Furrer, H.-U. Güdel, K. Krämer, H. Mutka, A. Wildes, K. Habicht, and P. Vorderwisch, *Nature (London)* **423**, 62 (2003).
- [11] M. Kofu, J.-H. Kim, S. Ji, S.-H. Lee, H. Ueda, Y. Qiu, H.-J. Kang, M. A. Green, and Y. Ueda, *Phys. Rev. Lett.* **102**, 037206 (2009).
- [12] M. Jaime, V. F. Correa, N. Harrison, C. D. Batista, N. Kawashima, Y. Kazuma, G. A. Jorge, R. Stern, I. Heinmaa, S. A. Zvyagin *et al.*, *Phys. Rev. Lett.* **93**, 087203 (2004).
- [13] Z. Wang, M. Schmidt, Y. Goncharov, Y. Skourski, J. Wosnitza, H. Berger, H.-A. K. von Nidda, A. Loidl, and J. Deisenhofer, *J. Phys. Soc. Jpn.* **80**, 124707 (2011).
- [14] M. Azuma, Y. Fujishiro, M. Takano, M. Nohara, and H. Takagi, *Phys. Rev. B* **55**, R8658 (1997).
- [15] A. Oosawa, T. Ono, and H. Tanaka, *Phys. Rev. B* **66**, 020405(R) (2002).
- [16] M. Cyrot, B. Lambert-Andron, J. L. Soubeyroux, M. J. Rey, Ph. Dehault, F. Cyrot-Lackmann, G. Fourcaudot, J. Beille, and J. L. Tholence, *J. Solid State Chem.* **85**, 321 (1990).
- [17] A. Nozaki, H. Yoshikawa, T. Wada, H. Yamauchi, and S. Tanaka, *Phys. Rev. B* **43**, 181 (1991).
- [18] F. Deslandes, A. I. Nazzal, and J. B. Torrance, *Physica C* **179**, 85 (1991).
- [19] J. Matsuno, Y. Okimoto, M. Kawasaki, and Y. Tokura, *Appl. Phys. Lett.* **82**, 194 (2003).
- [20] H. D. Zhou, B. S. Conner, L. Balicas, and C. R. Wiebe, *Phys. Rev. Lett.* **99**, 136403 (2007).
- [21] G. Jackeli and G. Khaliullin, *Phys. Rev. Lett.* **103**, 067205 (2009).

- [22] H. D. Zhou, Y. J. Jo, J. Fiore Carpino, G. J. Munoz, C. R. Wiebe, J. G. Cheng, F. Rivadulla, and D. T. Adroja, *Phys. Rev. B* **81**, 212401 (2010).
- [23] R. Viennois, E. Giannini, J. Teyssier, J. Elia, J. Deisenhofer, and D. V. der Marel, *J. Phys.: Conf. Ser.* **200**, 012219 (2010).
- [24] M. V. Eremin, J. Deisenhofer, R. M. Eremina, J. Teyssier, D. van der Marel, and A. Loidl, *Phys. Rev. B* **84**, 212407 (2011).
- [25] J. Teyssier, R. Viennois, E. Giannini, R. M. Eremina, A. Günther, J. Deisenhofer, M. V. Eremin, and D. van der Marel, *Phys. Rev. B* **84**, 205130 (2011).
- [26] T. Ueno, J. Kim, M. Takata, and T. Katsufuji, *J. Phys. Soc. Jpn.* **83**, 034708 (2014).
- [27] J. Bang, S. Matsuishi, H. Hiraka, F. Fujisaki, T. Otomo, S. Maki, J. Yamaura, R. Kumai, Y. Murakami, and H. Hosono, *J. Am. Chem. Soc.* **136**, 7221 (2014).
- [28] J. Teyssier, E. Giannini, A. Stucky, R. Cerný, M. V. Eremin, and D. van der Marel, *Phys. Rev. B* **93**, 125138 (2016).
- [29] W. Gong, J. E. Greedan, G. Liu, and M. Bjorgvinsson, *J. Solid. State Chem.* **95**, 213 (1991).
- [30] J. Deisenhofer, S. Schaile, J. Teyssier, Z. Wang, M. Hemmida, H.-A. K. von Nidda, R. M. Eremina, M. V. Eremin, R. Viennois, E. Giannini *et al.*, *Phys. Rev. B* **86**, 214417 (2012).
- [31] K. Momma and F. Izumi, *J. Appl. Crystallogr.* **44**, 1272 (2011).
- [32] We also performed the thermogravimetric analysis for the grown crystals and found that there is a variation of oxygen off-stoichiometry  $\delta$  for  $\text{Sr}_2\text{VO}_{4-\delta}$  from 0.1 to 0 depending on the sample, which is not correlated with the concentration of Ti or Nb. This does not seem completely consistent with the systematic change in the physical properties with the Ti or Nb doping as discussed below in the main text. At present, we do not fully understand how such oxygen off stoichiometry affects (or does not affect) the physical properties in orthorhombic  $\text{Sr}_2\text{VO}_{4-\delta}$ .
- [33] The reason of the factor of 2 difference between Eqs. (5) and (6) is as follows:  $N$  is the number of V ions and thus, the number of dimers is  $N/2$ . Since only one spin appears if one of the V ions is substituted by Ti, the number of the Curie-Weiss spins is given by the number of dimers  $N/2$  times the probability that one of the V ions is substituted by Ti,  $2x(1-x)$ . Accordingly,  $C_2$  is given by Eq. (5). On the other hand,  $C_1$  corresponds to the Curie constant in the high- $T$  limit of  $\chi_{SG}(T)$  given by Eq. (1) where there are two spins per dimer (one spin per V). Thus, the number of spins in total becomes the number of V ions  $N$  times the probability that neither V ion is substituted by Ti,  $(1-x)^2$ . Accordingly,  $C_1$  is given by Eq. (6).
- [34] The extrapolation of the reflectivity spectra outside the measurement range (0.05–5 eV) was performed irrespective of the Nb doping or polarizations as follows: Above 5 eV, we assume a constant reflectivity of 0.14 up to 20 eV, and then it is further extrapolated by an  $\omega^{-4}$  relation above 20 eV. Below 0.8 eV, we assume a constant reflectivity of 0.5 down to 0 eV.
- [35] M. M. Qazilbash, A. A. Schafgans, K. S. Burch, S. J. Yun, B. G. Chae, B. J. Kim, H. T. Kim, and D. N. Basov, *Phys. Rev. B* **77**, 115121 (2008).
- [36] K. Ohgushi, Y. Okimoto, T. Ogasawara, S. Miyasaka, and Y. Tokura, *J. Phys. Soc. Jpn.* **77**, 034713 (2008).
- [37] T. Katsufuji, Y. Taguchi, and Y. Tokura, *Phys. Rev. B* **56**, 10145 (1997).
- [38] J. Fujioka, S. Miyasaka, and Y. Tokura, *Phys. Rev. B* **72**, 024460 (2005).
- [39] A. Urushibara, Y. Moritomo, T. Arima, A. Asamitsu, G. Kido, and Y. Tokura, *Phys. Rev. B* **51**, 14103 (1995).